Available online at www.sciencedirect.com
ScienceDirect
Physica C 467 (2007) 167–173
PHYSICA C
www.elsevier.com/locate/physc

An EXAFS study of $RuSr_2GdCu_2O_8$: Evidence of magnetoelastic coupling

A. Paolone [a,b,*], C. Castellano [c], O. Palumbo [a,d], F. Cordero [e], R. Cantelli [a], A. Vecchione [b,f], M. Gombos [b,f], S. Pace [b,f], M. Ferretti [c,g]

[a] *Dipartimento di Fisica, Università di Roma "La Sapienza", Piazzale A. Moro 2, I-00185 Roma, Italy*
[b] *Laboratorio Regionale SuperMat, CNR-INFM, Salerno, Italy*
[c] *Laboratorio Regionale LAMIA, CNR-INFM, Corso Perrone 24, I-16152 Genova, Italy*
[d] *Consorzio Interuniversitario per le Scienze Fisiche della Materia – CNISM, Unità di Roma "La Sapienza", Dipartimento di Fisica, Piazzale A. Moro 2, I-00185 Roma, Italy*
[e] *CNR-ISC, Istituto dei Sistemi Complessi, Area della Ricerca di Roma-Tor Vergata, Via del Fosso del Cavaliere 100, I-00133 Roma, Italy*
[f] *Università di Salerno, Dipartimento di Fisica, Baronissi, Salerno, Italy*
[g] *Università di Genova, Dipartimento di Chimica e Chimica Industriale, Via Dodecaneso 31, I-16146 Genova, Italy*

Received 12 June 2007; accepted 2 October 2007
Available online 15 October 2007

Abstract

The EXAFS spectrum of two samples of $RuSr_2GdCu_2O_8$ prepared by means of slightly different procedures was measured in the temperature range from 10 up to 300 K on the K-edge of Cu. Both the basal and the apical Cu–O distances are not influenced by the magnetic and the superconducting transitions. Moreover the temperature dependence of the Debye–Waller factors of the $R(\text{Cu–O}_{\text{basal}})$ distance for both samples is in agreement with the Debye model for thermal disorder. On the contrary, $\sigma^2(\text{Cu–O}_{\text{apical}})$ shows a clear peak around the magnetic transition. This effect is attributed to magnetoelastic coupling.

PACS: 61.10.Ht; 75.30.−m; 75.80.+q

Keywords: Ruthenocuprates; Magnetoelastic coupling; EXAFS

1. Introduction

Superconductivity and magnetism are usually considered mutually exclusive, at least according to the BCS theory. However, the report of a magnetic transition (T_M) in ruthenocuprates at a temperature well above the superconducting critical temperature (T_C), $T_M/T_C \sim 3$, [1] posed new questions about the coexistence of superconductivity and magnetism. Most of the research on ruthenocuprates has been conducted on $RuSr_2GdCu_2O_8$, which has $T_C \sim 40$ K and $T_M \sim 135$ K. This compound has the same structure as YBCO, with Gd, Sr and Ru atoms replacing Y, Ba and Cu of the Cu–O chains [2], as reported in Fig. 1. The magnetic transition around 135 K is due to the order of Ru ions moments. Muon spin resonance measurements ensure that the magnetic ordering is indeed a property of the whole system and not only of a parasitic phase. Magnetization measurements show a ferromagnetic order, whilst neutron diffraction data give evidence of a predominant antiferromagnetic coupling. A possible explanation for this apparent discrepancy has been provided by Jorgensen et al. [3]: the dominant order of the Ru lattice is antiferromagnetic, with the easy axis oriented perpendicular to the Ru–O layers; however the whole subsystem is slightly canted resulting in a net ferromagnetic component along

* Corresponding author. Address: CNR-INFM, Dipartimento di Fisica, Università di Roma "La Sapienza", Piazzale A. Moro 2, I-00185 Roma, Italy. Tel.: +39 06 49914400; fax: +39 06 4957697.
E-mail address: annalisa.paolone@roma1.infn.it (A. Paolone).

0921-4534/$ - see front matter © 2007 Elsevier B.V. All rights reserved.
doi:10.1016/j.physc.2007.10.009

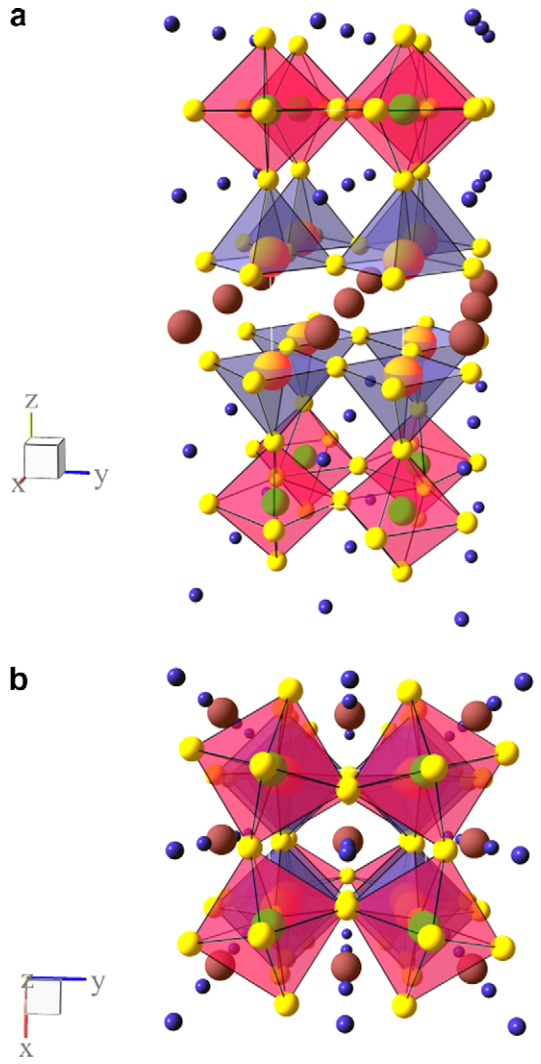

Fig. 1. The crystal structure of $RuSr_2GdCu_2O_8$, according to Ref. [2], projected along two different directions. The green, yellow, blue, orange and purple atoms are Ru, O, Sr, Cu and Gd, respectively. (For interpretation of the references to color in this figure legend, the reader is referred to the web version of this article.)

the *ab*-planes, that is observed by magnetization measurements. Below 2.6 K, also the Gd ions order antiferromagnetically, with the easy axis of the magnetization parallel to the *c*-axis [4]. The debate is still open on the real spatial coexistence of superconductivity and magnetism and on the microscopic order of Ru magnetic moments (for a review see Ref. [5]).

In the framework of the studies of the magnetic properties of $RuSr_2GdCu_2O_8$, the occurrence of magnetoelastic coupling has been suggested analysing the temperature behavior of the real part of the Young's modulus, E' [6]. Indeed in the paramagnetic phase E' decreases almost linearly with T, in agreement with the usual quasiharmonic approximation of the lattice dynamics described by the Debye model. However, around the ferromagnetic transition, E' is affected by the onset of the magnetic order, slightly decreasing from the expected Debye behavior down to about 90 K, suggesting magnetoelastic coupling.

In the present paper, we will present EXAFS measurements as a function of temperature on two samples of $RuSr_2GdCu_2O_8$ prepared by means of two slightly different procedures. Whilst no signature of the superconducting transition has been found, a marked increase of the Debye–Waller factors of the Cu–O bond-shell along the apical direction has been detected around the magnetic transition, indicating the occurrence of magnetoelastic coupling.

2. Experimental details

The $RuSr_2GdCu_2O_8$ samples were prepared by two slightly different methods reported in Refs. [7,8]. In both procedures polycrystalline samples of composition $RuSr_2GdCu_2O_8$ have been synthesized by solid state reaction of high purity stoichiometric powders of RuO_2, Gd_2O_3, CuO and $SrCO_3$. In the first method (sample obtained by this procedure will be labelled as G in the following) the mixture was first calcined in air at 950 °C; then, after grinding and die-pressing into pellets, it was treated in flowing N_2 atmosphere at 1010 °C. This step resulted in the formation of a mixture of the precursor materials Sr_2GdRuO_6 and Cu_2O without formation of the impurity phase $SrRuO_3$. The mixture was then subjected to eight successive sintering steps in flowing O_2, each one lasting 15 h, at temperatures starting from 1030 °C up to 1085 °C. Each successive thermal treatment was performed at a temperature 7 °C higher than the previous one. In the second procedure [8] (sample obtained by this procedure will be labelled as S in the following) stoichiometric amounts of Gd_2O_3, $SrCO_3$, RuO_2 and CuO were ball milled for 1 h and then calcinated in a muffle furnace for 10 h at 960 °C in air. About 5 g of the obtained powders have been pressed, by a uniaxial hydrostatic press, into a 5 cm (length) × 1 cm (width) × 0.4 cm (thickness) bar and then annealed in an horizontal furnace for 60 h in flowing Ar (1 atm, 20 l/h) at 1020 °C. The bar underwent subsequently two oxygenation cycles of 10 h and 60 h at 1020 °C in a horizontal furnace in flowing O_2 (1 atm, 20 l/h). Between the two oxygenation processes the bar was ground in an agate mortar and the powders were mixed for 1 h in a ball mill. X-ray diffraction pattern revealed that the powders were single phase.

The $RuSr_2GdCu_2O_8$ powders were dispersed in a cellulose matrix. Cu K-edge EXAFS data were recorded in transmission geometry and in the temperature range 10–300 K at the beamline E4 at the HASYLAB synchrotron radiation source (Hamburg) using an helium flux cryostat. The EXAFS oscillations $\chi(k)$ were extracted from the experimental data using standard procedures [9] and were normalized using the Lengeler–Eisenberger [10] method. Fig. 2 shows the $k\chi(k)$ signals at different temperatures between 10 and 298 K. The k^3 weighted $\chi(k)$ data were Fourier transformed (FFT) in the k range between 2.75 and 17.48 $Å^{-1}$. The obtained Fourier transform shows many correlation peaks up to $R = 6$ Å, as expected for an

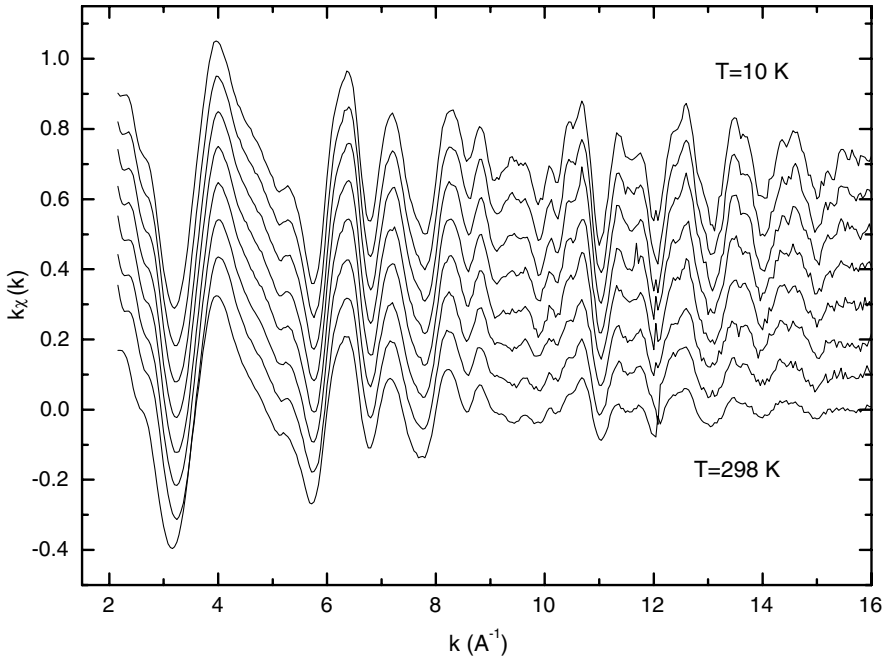

Fig. 2. k weighted EXAFS signals as a function of temperature for the G sample at (from bottom to top) $T = 298$, 250, 210, 150, 130, 100, 50 and 10 K.

ordered crystalline structure. The analysis was restricted to the first shell FFT peak, corresponding to the superposition of the Cu–O neighbors contributions, by inverse Fourier transforming (Fourier filtering) the data in the R range 1.05–2.12 Å. The filtered data were fitted using the standard single scattering EXAFS formula and theoretical amplitude and phase functions [11]. Two sub-shells were required to fit the data: one corresponding to $N(\text{Cu–O}_{\text{apical}}) = 1$ oxygen apical atom in the unit cell and the other corresponding to $N(\text{Cu–O}_{\text{basal}}) = 4$ oxygen basal atoms. This two sub-shells fit has been possible due to the extension of the data in the k range, to the windowing in the FFT space, to the number of independent fitting parameters and to the good signal-to-noise ratio. During the fit process, the coordination numbers $N(\text{Cu–O}_{\text{apical}})$ and $N(\text{Cu–O}_{\text{basal}})$ were fixed to the previous reported values. In this way the uncertainty on the mean square relative displacements of the bond lengths (or Debye–Waller factor), σ^2, was reduced. The fitting parameters were $\sigma^2(\text{Cu–O}_{\text{apical}})$, $\sigma^2(\text{Cu–O}_{\text{basal}})$ and the interatomic bond lengths for the two sub-shells. The interatomic distances used as starting points for the fit were the values obtained from previous neutron diffraction measurements [2] at room temperature: $R(\text{Cu–O}_{\text{basal}}) = 1.928 \pm 0.001$ Å and $R(\text{Cu–O}_{\text{apical}}) = 2.187 \pm 0.001$ Å. In Fig. 3 a typical example of the fit quality is shown.

3. Results and discussion

The results on the temperature dependence of the basal and apical Cu–O distances are shown in Fig. 4. In the G sample, the Cu–O distances in the plane and along the apical direction are constant within the experimental errors in the whole temperature range, with $R(\text{Cu–O}_{\text{basal}}) = 1.920 \pm 0.005$ Å and $R(\text{Cu–O}_{\text{apical}}) = 2.215 \pm 0.005$ Å, in agreement with the values reported by a combined high-resolution electron microscopy and synchrotron X-ray diffraction study [12]. Concerning the S sample, the basal bond length may be considered constant within the experimental errors with $R(\text{Cu–O}_{\text{basal}}) = 1.918 \pm 0.005$ Å. The apical Cu–O distance of the S sample shows an increase at 300 K consistently with a previous neutron diffraction study [2].

The temperature dependence of the Debye–Waller factors of the $R(\text{Cu–O}_{\text{basal}})$ distance for both samples is shown in Fig. 5. Both of them increase with increasing temperature, as expected considering the thermal disorder. In order to gain insight into the studied system, we considered that the Debye–Waller factor is the sum of a temperature independent static contribution, σ_s^2, and a temperature dependent dynamic contribution, σ_D^2, which can be expressed, according to the Debye model, as an infinite series whose first terms are [13]

$$\sigma_D^2 = \frac{3h^2}{Mk_B\theta_D}\left[\frac{1}{4} + \left(\frac{T}{\theta_D}\right)^2 \int_0^{\frac{\theta_D}{T}} dx \frac{x}{e^x - 1}\right]$$

where M is the mass of the diffuser atom and θ_D is the Debye temperature. The above formula shows that, once the mass of the atoms is known, σ_D^2 is a function of the Debye temperature alone. The best fit curves of the two Debye–Waller factors are reported in Fig. 5. In the case of sample G a good quality fit was obtained with $\theta_D = 390$ K, which fairly agrees with the value deduced by specific heat measurements [14] and Young's modulus measurements [6], and $\sigma_s^2(\text{Cu–O}_{\text{basal}}) = 0.0047$ Å^2. For sample S a lower

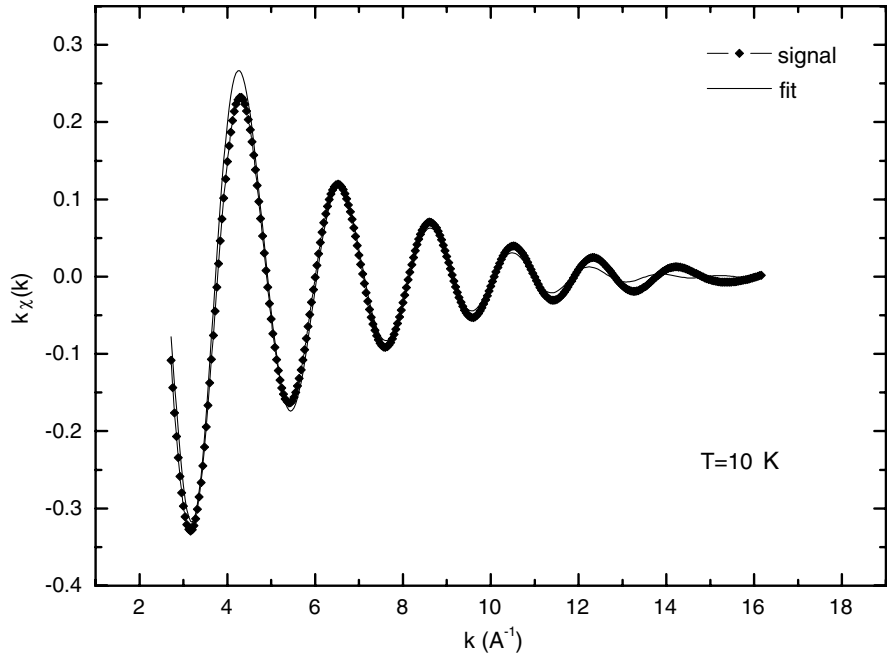

Fig. 3. IFT XAFS signal for the G sample at $T = 10$ K (symbols) and the best fit curve obtained with the two sub-shells model (line).

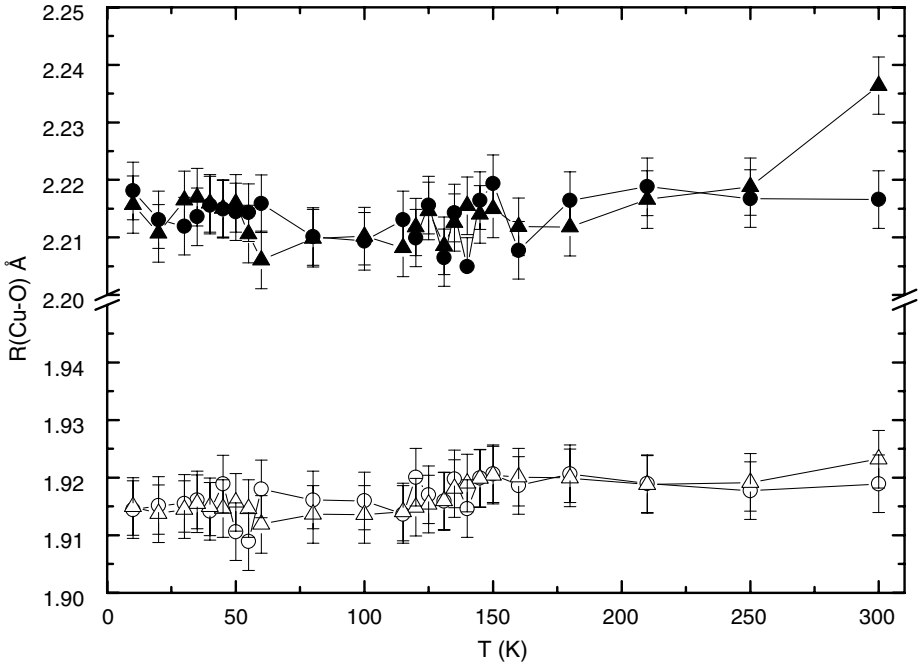

Fig. 4. Temperature dependence of the basal (empty symbols) and apical (full symbols) Cu–O distances for the G (circles) and S (triangles) sample.

quality fit was obtained with $\theta_D = 405$ K and $\sigma_s^2(\text{Cu–O}_{\text{basal}}) = 0.0044$ Å^2. One can note that there are no signatures of the superconducting or of the magnetic transition.

In Fig. 6 the temperature dependence of the Debye–Waller factor of the distance between Cu and the apical oxygen is reported for both samples. A behavior clearly different from that expected for thermal disorder is evident. Indeed, in both samples σ^2 decreases with decreasing T from 300 K to 150 K; on further cooling σ^2 reaches a maximum at ~140 K in sample G (~130 K in sample S) and then decreases to very low values. Considering that the temperature range in which the deviation of σ^2 from the Debye model is observed is that of the magnetic transition, we propose that this unusual behavior of σ^2 is due to magnetoelastic coupling. Indeed the apical oxygen is chemically bound on one side to Cu and on the opposite side to Ru (see Fig. 1), whose magnetic moments order below $T_M \sim 135$ K. In a simple picture of magnetoelastic-

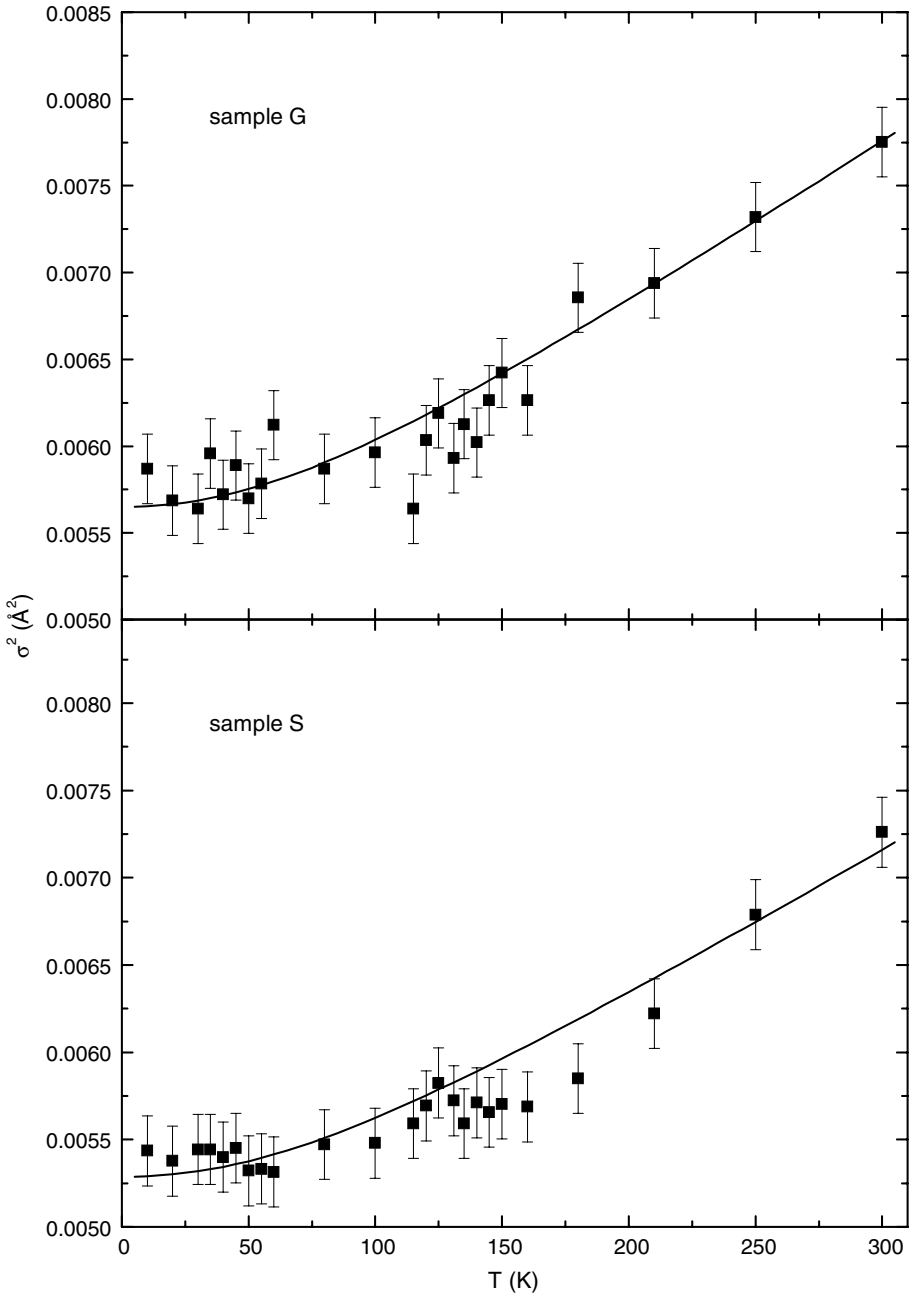

Fig. 5. The temperature dependence of the Debye–Waller factors of the in plane Cu–O distances for the two samples of $RuSr_2GdCu_2O_8$ (symbols) and the best fit curves.

ity, when a magnetic field develops in a material, there are both a volume and a shape variation of the sample due to the dependence of the exchange integral and of the interatomic distances on the magnetization. An abrupt change of the interatomic distance and a divergent behavior of the Debye–Waller factor for the nearest neighbor Fe–N shell were clearly observed by EXAFS measurements [15] on $[Fe(4\text{-amino-}1,2,4\text{-triazole})_3[CH_3SO_3]_2 \cdot 2H_2O$, which presents a spin-crossover phase transition at ~280 K. The peak of the Debye–Waller factor has been attributed to the very large difference between the low-spin and the high-spin states. In the case of ruthenocuprates, neutron diffraction data give evidence of a predominant antiferromagnetic coupling with the easy axis oriented perpendicular to the Ru–O layers. On the average, the sample size should not vary at T_M as alternate expansions and contractions of the $Ru–O_{apical}$ distances due to magnetoelastic coupling are expected. However a peak in the Debye–Waller factor around T_M can be understood as due to the occurrence of different $Ru–O_{apical}$ interatomic distances, which in turn gives rise to different $Cu–O_{apical}$ bond lengths. The lack of signatures of the magnetic phase transition in the Debye–Waller factor of the $Cu–O_{basal}$ distance is consistent with the fact that

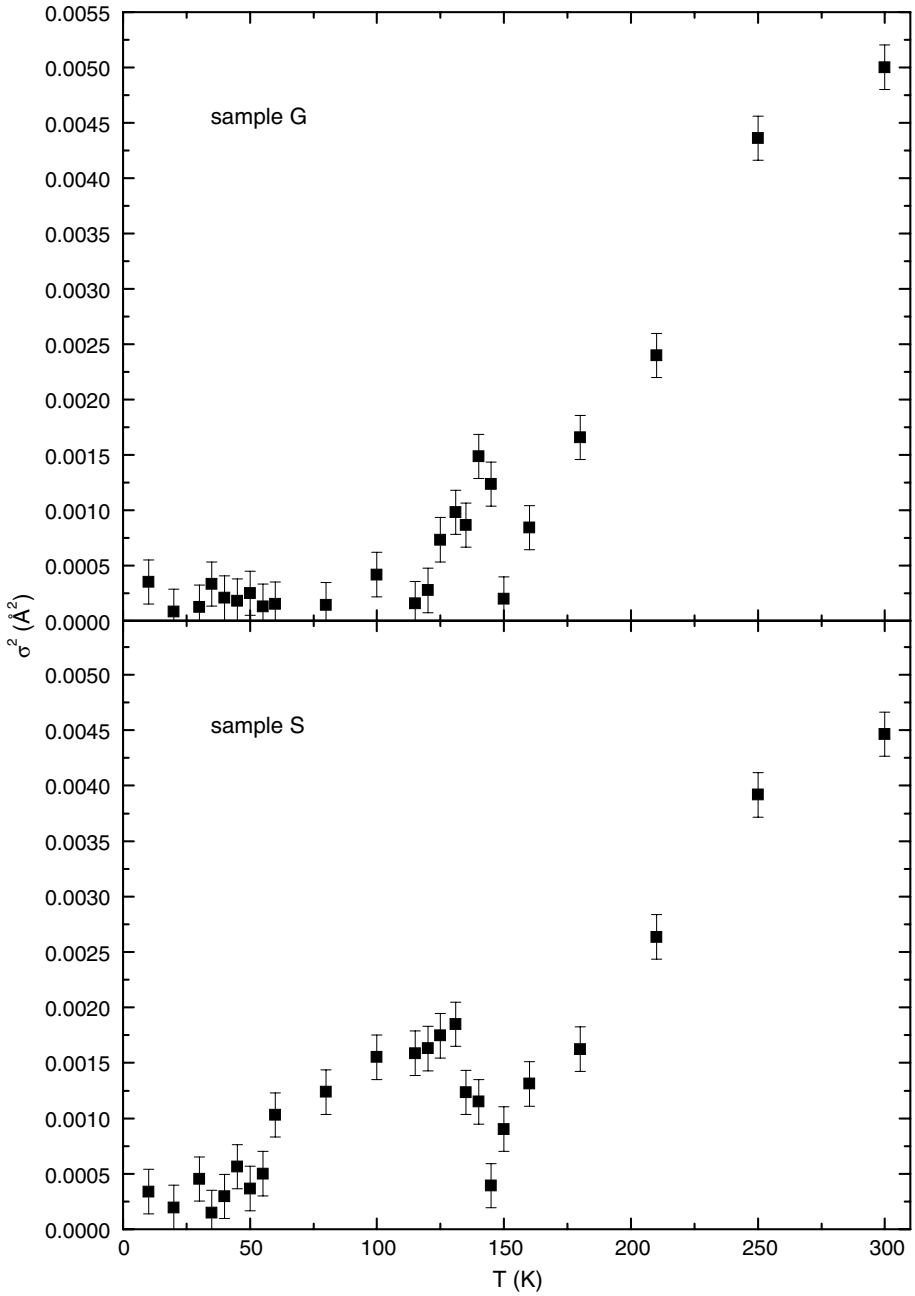

Fig. 6. The temperature dependence of Debye–Waller factor of the distance between Cu and the apical oxygen for the two $RuSr_2GdCu_2O_8$ samples.

the Ru magnetic moments are mainly aligned along the *c*-axis.

Previous neutron diffraction experiments detected an unexpected and anomalous structural change at the magnetic transition [2]. Indeed whilst the mean Cu–O and Ru–O distances had a regular behavior as a function of T, the Cu–Cu distance and the CuO_2 buckling angle exhibited two distinct linear responses above and below T_M. The authors of Ref. [2] suggested hybridization of the Ru and Cu electronic states as responsible for this behavior.

A last remark concerns the extremely low values of $\sigma^2(Cu–O_{apical})$ at temperatures much lower than T_M for both samples of ruthenocuprates. A similar effect has been observed in maganites below the ferromagnetic transition, where fits to a correlated Debye model require an unphysical, negative static distortion [16]. The decrease of the distortions at T_C were attributed to a charge localization mechanism due to Jahn–teller effect [16]. In ruthenocuprates poor information is available about possible Jahn–Teller effect, even if some authors [17] suggested it could be present.

4. Conclusions

Previous neutron diffraction measurements on $RuSr_2GdCu_2O_8$ reported an anomalous structural change at the

magnetic transition of the Cu–Cu distance and the CuO_2 buckling angle. In the present paper we report a study of the local structure of $RuSr_2GdCu_2O_8$ measured by means of EXAFS in the temperature range from 10 up to 300 K. Neither the basal nor the apical Cu–O distances are influenced by the magnetic and the superconducting transitions, and $\sigma^2(Cu–O_{basal})$ is well described by the Debye model for thermal disorder. However the Debye–Waller factor of the $Cu–O_{apical}$ bond shows a behavior clearly different from that expected for thermal disorder. Indeed, σ^2 decreases with decreasing T from 300 K to 150 K; on further cooling σ^2 reaches a maximum at $\sim$130–140 K and then decreases to very low values. This peak is attributed to magnetoelastic coupling.

Acknowledgements

We thank N.L. Saini for useful discussions and K. Klementiev for technical support at HASYLAB. This work was supported by the European Community – Research Infrastructure Action under the FP6 "Structuring the European Research Area" Programme (through the Integrated Infrastructure Initiative "Integrating Activity on Synchrotron and Free Electron Laser Science"), Contract RII3-CT-2004-506008.

References

[1] I. Felner, U. Asaf, Y. Levi, O. Millo, Phys. Rev. B 55 (1997) R3374.
[2] O. Chmaissem, J.D. Jorgensen, H. Shaked, P. Dollar, J.L. Tallon, Phys. Rev. B 61 (2000) 6401.
[3] J.D. Jorgensen, O. Chmaissem, H. Shaked, S. Short, P.W. Klamut, B. Dabrowski, J.L. Tallon, Phys. Rev. B 63 (2001) 054440.
[4] J.W. Lynn, B. Keimer, C. Ulrich, C. Bernhard, J.L. Tallon, Phys. Rev. B 61 (2000) R14964.
[5] T. Nachtrab, C. Bernhard, C. Lin, D. Koelle, R. Kleiner, CR. Phys. 7 (2006) 68.
[6] A. Paolone, F. Cordero, R. Cantelli, G.A. Costa, C. Artini, A. Vecchione, M. Gombos, J. Magn. Magn. Mater. 272–276 (2004) 2106.
[7] C. Artini, M.M. Carnasciali, G.A. Costa, M. Ferretti, M.R. Cimberle, M. Putti, R. Masini, Physica C 377 (2002) 431.
[8] A. Vecchione, M. Gombos, P. Tedesco, A. Immirzi, L. Marchese, A. Frache, C. Noce, S. Pace, Int. J. Mod. Phys. B 17 (2003) 899.
[9] P.A. Lee, P.H. Citrin, P. Eisenberger, B.M. Kinkaid, Rev. Mod. Phys. 53 (1981) 769.
[10] B. Lengeler, P. Eisenberger, Phys. Rev. B 21 (1980) 4507.
[11] A.G. McKale, J. Am. Chem. Soc. 110 (1988) 3763.
[12] A.C. McLaughlin, W. Zhou, J.P. Attfield, A.N. Fitch, J.L. Tallon, Phys. Rev. B 60 (1999) 7512.
[13] G. Beni, P.M. Platzman, Phys. Rev. B 14 (1976) 1514.
[14] J.L. Tallon, J.W. Loram, G.V.M. Williams, C. Bernhard, Phys. Rev. B 61 (2000) R6471.
[15] T. Yokoyama, Y. Murakami, M. Kiguchi, T. Komatsu, N. Kojima, Phys. Rev. B 58 (1998) 14238.
[16] C.H. Booth, F. Bridges, G.H. Kwei, J.L. Lawrence, A.L. Cornelius, J.J. Neumeier, Phys. Rev. B 57 (1998) 10440;
P.G. Radaelli, G. Iannone, M. Marezio, H.Y. Hwang, S.-W. Cheong, J.D. Jorgensen, D.N. Argyriou, Phys. Rev. B 56 (1997) 8265;
P. Dai, J. Zhang, H.A. Mook, S.-H. Liou, P.A. Dowben, E.W. Plummer, Phys. Rev. B 54 (1996) R3694.
[17] R.S. Liu et al., Phys. Rev. B 63 (2001) 212507;
R.S. Liu et al., Phys. Rev. B 65 (2002) 064508.